Sun, Jiyu, Wu, Wei, Song, Zelai, Tong, Jin and Zhang, Shujun ORCID logoORCID: https://orcid.org/0000-0001-5699-2676 (2019) Bio-inspirations for the Development of Light Materials based on the Nanomechanical Properties and Microstructures of Beetle Dynastes tityus. Journal of Bionic Engineering, 16 (1). pp. 154-163. doi:10.1007/s42235-019-0014-7

Official URL: http://dx.doi.org/10.1007/s42235-019-0014-7
DOI: http://dx.doi.org/10.1007/s42235-019-0014-7
EPrint URI: https://eprints.glos.ac.uk/id/eprint/6417

Journal of Bionic Engineering (2019) DOI: https://doi.org/12345-018-1234-x

Bio-inspirations for the Development of Light Materials based on the Nanomechanical Properties and Microstructures of Beetle *Dynastestityus*

Jiyu Sun[1*], Wei Wu[1], Zelai Song[1], Jin Tong[1], Shujun Zhang[1,2*]

1. *Key Laboratory of Bionic Engineering* (*Ministry of Education, China*), *Jilin University, Changchun* 130022, *China*

2. *School of Computing and Technology, Gloucestershire University, Cheltenham GL*50 2*HR, UK*

Abstract

Dynastes tityus (*D. tityus*) is a typical beetle whose elytra are light and strong. The primary function of elytra is to protect beetle's hindwings. In this paper, *D. tityus* elytra were selected as the biological prototype for the investigation to obtain bio-inspirations for the design and development of light materials with high ratio of strength to mass. Firstly, the microstructure investigation and quasi-static nanoindentation tests have been carried out on the ten samples of the selected elytra of *D. tityus* to reveal their mechanical properties and microstructures. Secondly, based on the findings from the microstructure investigation and nanoindentation tests, three models of bio-inspired materials have been proposed for further study to gain the deep understanding of the relationships between the special mechanical characteristics and microstructures. Then Finite Element Analysis (FEA) simulations have been performed on the three models for harvesting the bio-inspirations for the initial design of light materials. Finally, through comparative analysis of the findings from the microstructure investigation, the nanoindentation tests and the simulations, some meaningful bio-inspirations have been reaped for the future optimization of the design and development of light materials with high ratio of strength to mass.

Keywords: beetle elytra, bio-inspirations, nano-mechanical properties, microstructures, light-weight materials with high strength

1 Introduction

It has been widely accepted that the functional and mechanical properties of biological bodies are enriching for the design and development of bionic materials. The fore wings (elytra) of *Coleoptera* (popularly called beetles) are relatively strong with the main function of protecting the hind wings and abdominal spiracles, and controlling water loss[1]. It has been found that the microstructures of the elytra of beetles can contribute to the formation of their efficient exoskeleton of lightweight and high strength[2]. The beetle elytron cuticle is a laminated structure consisting of chitin fibers and a proteinaceous matrix[3]. The comparison of mechanical properties between Beetle Elytron Plates (BEPs) and Honeycomb Plates (HPs) shows that mechanical strength of BEPs are several times higher than that of the HPs[4]. The biomimetic models based on *Allomyrina dichotoma* indicates that the spiral-type model has good mechanical properties when stretched or sheared, whereas the linear-type model performs well when compressed[5] and the T-shaped fiber structures within *Trigonophorus flammea* elytra increase their bending strength[6]. Under both compression and three-point bending conditions, the spherical chamber structure designed from *Cybister tripunctatus orentalis Gschew* displays the better specific strength and specific stiffness than that honeycomb structure from *Trypoxylus dichotomus*[7].

Some bioinspired composite materials based on beetle's elytra have been designed and fabricated. Bioinspired lightweight structures with cavities and hollow columns were designed and built from acrylonitrile butadiene styrene plastic with a three-dimensional printer[8]. A bionic bi-tubular thin-walled structure was inspired from the internal structure of the lady beetle elytron, and the single-wall tubes were prepared using aluminum alloy[9]. While their parameters used in simulation are uniform value or acquired by tensile testing, mechanical properties of the biomaterials are varied within different parts or segments. The presence of the trabeculae and border structures of *A. dichotoma* gives elytra sufficiently flexural, compressive strength and effectively increases the peel strength between the upper and lower laminations of elytra, while the characteristic overlay angles between the fiber layers of the upper lamination and the variable cross-section confers the mechanical properties required for flight[10].

The mechanical behaviors of insect cuticles have been studied using micro-tensile testing and fracture testing[11,12]. While chitin fibers and proteinaceous matrix in cuticles are known to be micro or nano-scale, so traditional mechanical testing techniques can't provide valuable mechanical information. Nanoindentation, a new technique, can probe the nanomechanical properties of both micro- and nano-sized materials. It has been used to investigate the mechanical properties of the human tooth, cuticle, and dragline silk[13–15]. Additionally, it has also been found that the water content and tanning will effect on mechanical properties[16,17]. To obtain deep and comprehensive understanding of the mechanical properties of the beetle elytron for harvesting meaningful bio-inspirations, both the micro- and nanomechanical properties should be investigated.

Beetle *Dynastes tityus* (*D. tityus*) is an interesting insect that its elytra are not only light with relatively high strength for protecting hindwings and body, but also can reversibly change color from green to black when the environmental humidity increases. It has been found that the color-changing feature of *D. tityus* elytron is related to its photonic crystal microstructure[18].

The above special functional and structural features of *D. tityus* elytra assure it is an ideal biological prototype for obtaining the bio-inspirations for the design and development of materials that are not only light and strong, but also with color-changing capability. Due to the limitation of the time and space and considering the fact that the structure and mechanical properties are critical to any materials. In this paper, the focus is placed on the investigation of the structure, mechanical property and their relationships to obtain the bio-inspirations for designing and developing bio-materials that are light in weight and high in strength.

In this paper, in sections **2** and **3**, both the microstructure investigation and the quasi-static nanoindentation will be firstly carried out on the ten samples of the selected elytra of *D. tityus* to reveal their mechanical properties and microstructures. Based on the findings from the nanoindentation tests, in section **4**, three models of bio-inspired materials will be then proposed for further study to gain the deep understanding of the relationships between the special mechanical characteristics and microstructures. After that, a number of Finite Element Analysis (FEA) simulations will be performed on the three models for harvesting the bio-inspirations for the future design and development of the light materials. Finally, through comparative analysis of the findings from the microstructure investigation, the nanoindentation tests and the simulations, some meaningful bio-inspirations will be reaped for the future optimization of the design and development of light materials with high ratio of strength to mass.

2 Materials and methods

2.1 Specimens

D. tityus beetles were caught in Shanghai, China. All the beetles studied are adults and 10 samples are used in our tests. The specimens are cut with a sharp knife near the highest point of the elytron for microstructure analysis and nanoindentation.

2.2 Microstructure investigation

For investigating the microstructure, the elytra specimens are cut into ultra-thin sections with length of 0.35 mm – 0.4 mm, width of 0.17 mm – 0.2 mm and thickness of 70 nm by ultramicrotome (EM UC7, LEICA, Germany). The machine accuracy is 40 nm. The microstructures of Transverse Direction (TD) and Longitudinal Direction (LD) of the cut sections are recorded by a multiplication microscope (Scope.A1, ZEISS, Germany). The machine resolution is 0.25 μm. The details of fibers and layers of the elytra section are acquired by the Environmental Scanning Electron Microscope (ESEM; JEOL JSM-6700F, FEI Company, USA).

2.3 Nanoindentation

For nanoindentation tests, the specimens are embedded in GD301-A/B epoxy resin as a supporting foundation during testing. Each specimen is measured 10 times. Since the curvature of beetle elytra is very big and length is small in the transverse direction, so in this paper, the tensile testing is carried out in the longitudinal direction for acquiring micromechanical properties.

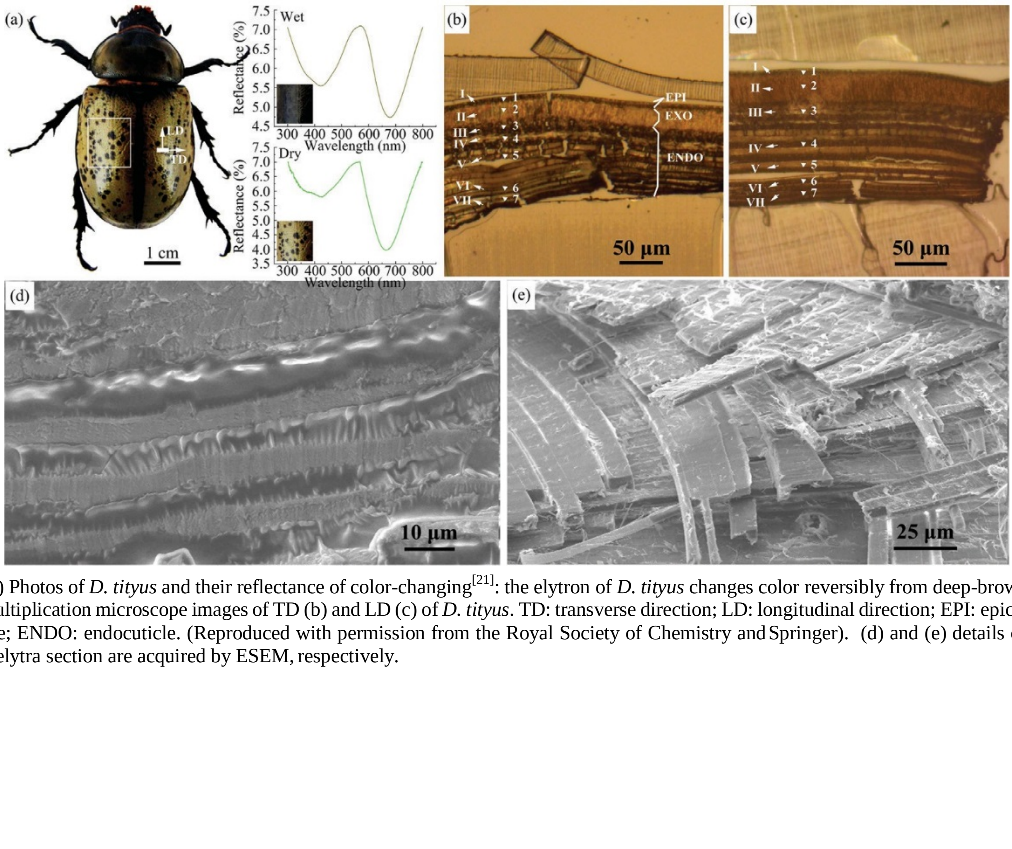

Fig. 1 (a) Photos of *D. tityus* and their reflectance of color-changing[21]: the elytron of *D. tityus* changes color reversibly from deep-brown to yellow-green. Multiplication microscope images of TD (b) and LD (c) of *D. tityus*. TD: transverse direction; LD: longitudinal direction; EPI: epicuticle; EXO: exocuticle; ENDO: endocuticle. (Reproduced with permission from the Royal Society of Chemistry and Springer). (d) and (e) details of layers and fibers of elytra section are acquired by ESEM, respectively.

To investigate the nanomechanical properties, a nanoindenter (TriboIndenter, Hysitron Inc., USA) is used on TD and LD of *D. tityus* elytra. A Berkovich tip is chosen for quasi- static nanoindentation. A typical trapezoidal loading function is applied to minimize the effects of the visco-elastic properties of biomaterials on the testing results for the biomaterial indentation tests[19]. The test parameters are: peak load of 500 μN, loading rate of 50 $\mu N \cdot s^{-1}$, and holding time of 10 s. The Oliver-Pharr method is adopted to determine the reduced modulus (E_r) and hardness (H), they can be expressed as[20]:

$$\frac{1}{E_r} = \left(\frac{1-v^2}{E}\right)_{\text{specimen}} + \left(\frac{1-v^2}{E}\right)_{\text{indenter}}, \tag{1}$$

$$H = \frac{P_{\max}}{A(h_C)}, \tag{2}$$

$$E_r = \frac{\sqrt{\pi}}{2\beta}\frac{S}{\sqrt{A(h_c)}}, \tag{3}$$

where, v is Poisson's ratio, $A(h_C)$ is the projected contact area between the tip and the sample surface, P_{max} is the maximum indentation force, S is experimentally measured stiffness of the upper portion of the unloading data, β is a constant related to the tip geometry, is 1.034 for the Berkovich tip.

3 Test results

3.1 Microstructure

The results of the microstructure investigation reveal that:

(1) The structures of the TD and LD vary, but similar to each other as shown in Figs.1b and 1c, which demonstrates that the elytra of *D. tityus* are anisotropy.

(2) The elytra of *D. tityus* are consist of seven layers. On the top is epicuticle (EPI), called layer I. In layer I, the material is in sponge-like microstructure. Under layer I, there is a layer of exocuticle (EXO), called layer II. The material in this layer is photonic crystals with porous microstructure. With this special microstructure, the elytra of *D. tityus* can change its color, for example from deep brown at a relative humidity of 98% to yellow green at a relative humidity of 34% as shown in Fig. 1a[21].

(3) After layer II is the area filled with the endocuticle (ENDO). There are five layers in this area, called layers III, IV, V, VI and VII, respectively. Layers III to VII are the laminated structures with different thicknesses and modulus, which ensure elytra's stiffness.

(4) For each layer, there are numerous serrations that are relatively evenly distributed on the surfaces. The details of connections between layers are shown in Fig. 1d. Elytra are composed by protein matrix and chitin fibers. From the Fig. 1d, it can be observed that there are fibers that stick out of the layer surfaces. So it is believed that the bonding force between layers depends on the friction of these fibers. There are no other materials bonding the layers. This is different from most existing man-made composite materials.

(5) In each layer there are also some strips of fibers bundles (Fig. 1e). The geometrical orientations of these strips of fiber bundles show a variance. The orientation angles are different between two adjacent layers. The strips intersect in various directions. This special geometrical configuration increases the contact area between fibers and matrix. So, the bonding force between fibers and matrix is increased. Besides, the greater bonding force, the greater friction force between fibers and ultimately, the stronger elytra.

In summary, like the other insect cuticles, the elytra of *D. tityus* can be considered as a composite consisting of chitin fibers, fiber bundles and a proteinaceous matrix in a layered structure, which is in the concordance with the findings of the researches by Refs. [22,23].

3.2 Nanoindentation

Fig. 2 shows the results of quasi-static nanoindentation. Figs. 2a and 2b show E_r and H of the elytra of *D. tityus* in both TD and LD for each layer from EPI to ENDO. The results of the nanoindentation tests show that:

(1) Both E_r and H display fluctuant variations. E_r and H in TD are higher than those in LD.

(2) The relatively low strength at the surface of the elytra plays a buffer role, and then the higher strength in inner layers helps to maintain its shape and stability. E_r and H of point 5 in TD are 51.29% and 69.1%, respectively, higher than those of point 1. Similarly, in LD, E_r and H of point 5 are 88.5% and 29%, respectively, higher than those of point 1. E_r and H at point 2 in TD and at point 4 in LD are the lowest due to the indentation at the weakest positions. Additionally, the E_r and H at point 6 are low and similar to those at point 1. The reason for these findings is possibly due to the fact that points 1 and 6 are near the surface of the front and the back of the elytra.

(3) Another finding is that the material elasticity of the whole elytron is distributed in optimum way. This special microstructure can be one of the essential mechanisms to make it is difficult to break the elytra. This finding can be evidenced by the previous research findings that many biomaterials are strong and have fibers that are aligned in certain directions and are anisotropic[12,24,25]

(4) The protein matrix in TD may also be the reason why the cuticle hardens and displays anisotropic properties. This mechanical property of the insect cuticle may provide important bio-inspirations for the design of light composites with high ratio of strength to mass.

(5) As discussed above, the elytra of *D. tityus* are anisotropy and E_r and H are different in TD and LD. In addition, E_r and H are also not same in different positions from layers to layers (from EPI to ENDO). However these findings have not been considered in the previous bioinspired models or materials, which is possible the reason why there are clear deviations between the mechanical properties of the reported bioinspired materials and biological prototypes. This is another important bio-inspiration for the design and development of future bio-inspired composite materials, that is the E_r and H should be distributed in optimum way not only in different directions of the sections, but also in the different positions on the sections.

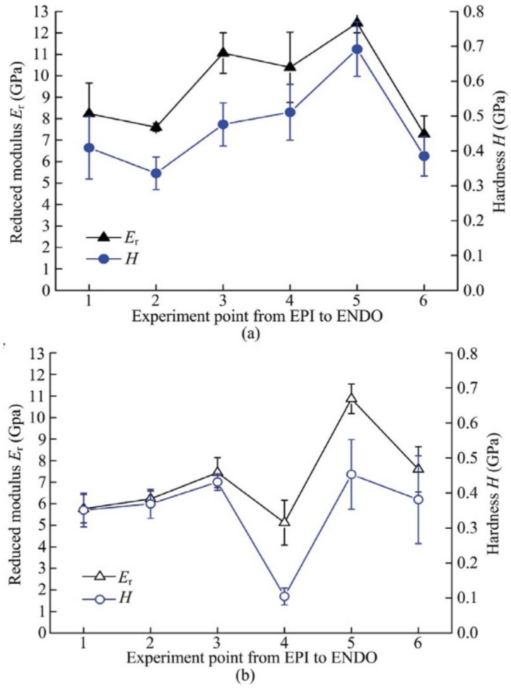

Fig. 2 Nanoindentation testing results of the elytra. (a) and (b) present the results for the TD and LD of *D. tityus*, respectively.

4 Bioinspired models

In this section, based on the findings from both the microstructure investigation and the nanoindentation tests, three models of bio-inspired materials will be proposed for further study using FEA to gain the deep understanding of the relationships between the special mechanical characteristics and microstructures and to continuously harvest the bio-inspirations for light and strong material design and development.

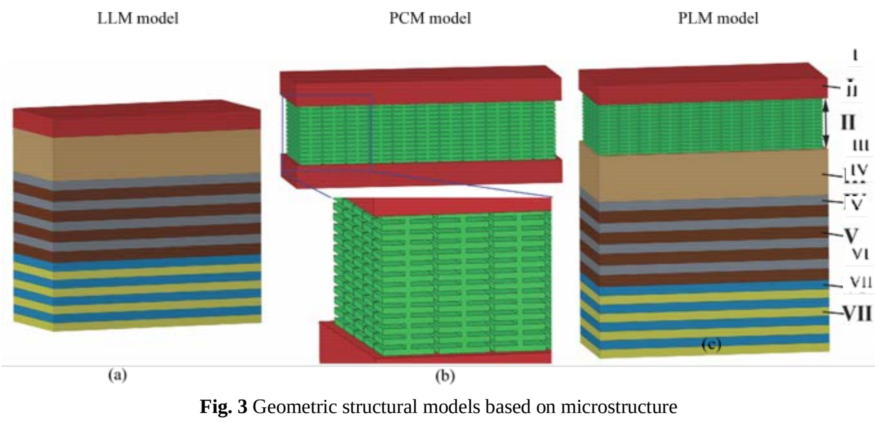

Fig. 3 Geometric structural models based on microstructure

Considering the nanomechanical properties and microstructures of 7 layers of the elytra, three bio-inspired models of composite materials have been proposed: the Photonic Crystal Model (PCM), the Laminated Layer structure Model (LLM) and the combined model of photonic crystal and laminated layer structures (PLM), shown in Fig. 3. PCM model is consist of layers I and II with purpose of investigating the effects of the first layer materials and microstructures (EPI and photonic crystal) on the strength of the elytra and the mechanisms of color changes. LLM model is consist of layer I and layers III to VII with purpose of investigating the effects of only laminated structure of layers on the strength of the elytra. The combined model, PLM is consisting of all 7 layers with purpose of evaluating the effects of all found materials and microstructures on the strength of the elytra. As shown in Fig. 3, layers I–VII are presented in the different colors.

For the simulation purposes, layers I to VII are given the different thicknesses and modulus as listed in Table 1. However, the material property, E_r is kept same for the same layer. The weights of PLM and PCM models have been evaluated using CERO software and found that they are 10.56% and 29.5% lighter than LLM, respectively. This is due to the fact that both PLM and PCM models have a layer of photonic crystal.

Table 1 The parameters for each layer of the coupled structure- nanomechanical models

Layers	Thickness (μm)	E_r of TD (MPa)	E_r of LD (MPa)
I	8.04	8.00×10^3	5.70×10^3
II	21.40	7.50×10^3	6.20×10^3
III	18.50	1.10×10^4	7.50×10^3
IV	3.86	1.05×10^4	5.10×10^3
V	4.70	1.25×10^4	1.10×10^4
VI	3.69	7.50×10^3	7.50×10^3
VII	3.52	1.05×10^4	5.10×10^3

5 FEA simulation

FEA simulation can be used to reveal physical systems with geometry and load conditions using mathematical approximation. The solution domain consists of numerous small interconnecting sub-domains called finite elements, and the physical systems will be simulated by calculating the whole domain. This simulation method can adapt to various complicated shapes with high accuracy in engineering analysis of mechanical manufacturing, material processing, aerospace, automobiles, civil construction, electronics, military industry, ships, railways, petrochemicals and energy *etc*. So in this paper, FEA is applied to the three proposed models in section **4** to harvest further bio-inspirations for the design and development of future light and strong materials.

5.1 FEA parameters

For FEA simulation, the same uniform load of 500 μN is applied as that for the nanoindentation test. So, the total loads for FEA simulation are 0.5 MPa. In the analysis of the models under the compression, an even distributed load is applied on the top surface of each model. The total compression load is also 0.5 MPa. In addition, the last layer of each model is fixed on the stable horizontal surface. In tensile analysis, axial loads of 0.5 MPa are applied in the normal directions to the cross-sections of the model and this tensional force is symmetrically applied in opposite directions at each end cross-section of the module. In triangle indentation analysis, cycle vertical loads of 0.5 MPa are applied on the top of each model at the rate of 0.05 $MPa \cdot s^{-1}$ with a 10 s holding time. The last layer of each model is also fixed on the stable horizontal surface.

5.2 Simulation results

The strain and stress results under the compression, tensile and triangular indentation of the three models are presented in Fig. 4. Fig. 4a shows that the stresses and strains in both TD and LD for the three models under the even distributed pressure load of 0.5 MPa. From the figure, it can be found that:

(1) The maximum stresses for PCM (12.01 MPa and 12.29 MPa in TD and LD, respectively) are larger than those for PLM (11.60 MPa and 11.87 MPa in TD and LD, respectively). The maximum stress only occurs at the photonic crystal structure of these two models. The maximum stresses for LLM are 86.47% and 88.29% smaller than those for PLM in TD and LD, respectively. Being different from PCM and PLM, the maximum stress of LLM occurs at the corners of last layers in both TD and LD.

(2) However, in the whole volumes of LLM models, the minimum stresses are 0.25 MPa and 0.26 MPa in TD and LD, respectively, much higher than those for PCM (1.21×10^{-3} MPa and 1.26×10^{-3} MPa in TD and LD, respectively) and for PLM (1.48×10^{-3} MPa and 1.44×10^{-3} MPa in TD and LD, respectively).

(3) As expected, the maximum strains in TD and LD for both PCM and PLM occur in the photonic crystal structure as

well. The maximum strains of PLM are1.55×10^{-3} in TD and 1.91×10^{-3} in LD. They are 90.39% and 85.71% higher than those for LMM, respectively.

(4) However, the pressure loads have the limited influences on the structure below the photonic structure for PLM. The strains in layers III to VII are 2.41×10^{-7} in TD and 2.85×10^{-7} in LD and 99% and 99.33% less than those for LLM, respectively. The reason for this interesting phenomenon is that in PLM there is the photonic crystal layer that supports and absorbs pressure force. The same phenomenon has been observed for PCM.

(5) Young's modulus of layers I and are similar to each other.

(6) The strain and stress in the LLM are distributed uniformly throughout almost the whole model. This behavior may be due to the layer structure with same Young's modulus for all the layers.

The stress and strain of the tensile simulations of the three models are shown in Fig. 4b. From the figure, it can be seen that:

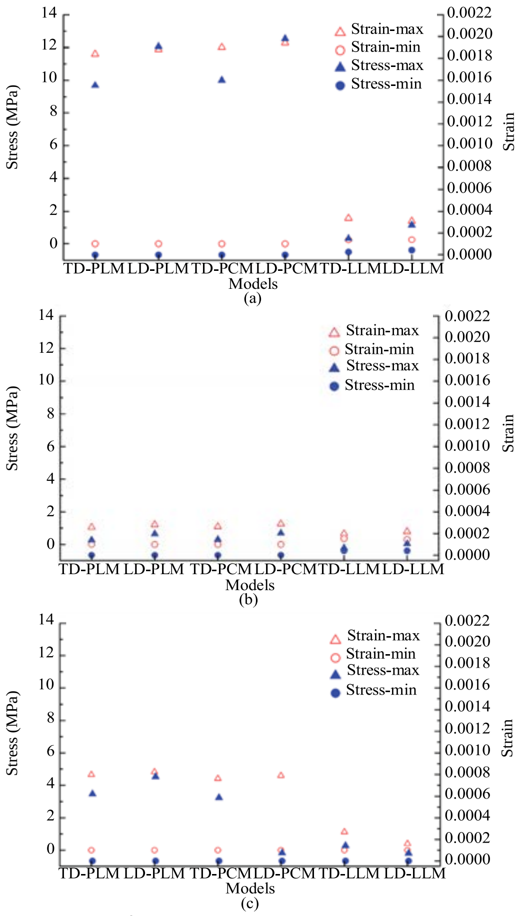

Fig. 4 Simulation results of the maximum and minimum for strain and stress under the compression (a), tensile (b) and triangular indentation (c).

(7) The maximum stresses for PLM and PCM occur at the connection are as between layer I and layer II (photonic crystals). These connection areas are the weakest parts in the whole models. It is interesting that the whole layer II shows the minimum stress. Thus, the tensile loads have the limited effects on the photonic crystal structure for PLM and PCM models.

(8) The maximum stresses for both PCM and PLM models are 1.09 MPa in TD and 1.05 MPa in LD, and 1.22 MPa in TD and 1.26 MPa in LD, respectively. The stress distributions in both TD and LD are similar to each other.

(9) The maximum strains of the PCM and PLM occur in the top layer of the connection areas between layer I and layer II (photonic crystals). The maximum strains of PCM and PLM are 1.45×10^{-4} and 1.40×10^{-4} in TD, and 2.03×10^{-4} and 1.97×10^{-4} in LD, respectively. However, the maximum strain of the LLM model occurs at the corner in the middle of the model with a value of 6.82×10^{-5} for TD, and 1.06×10^{-4} for LD, respectively. These strain distributions also depend on each layer's Young's modulus and the maximum strain always occurs in the layer with the smallest modulus.

(10) The whole LLM models in TD and LD display high stress distributions with the minimum stresses of 0.36 MPa and 0.30 MPa and the minimum strain of 4.09×10^{-5} and 4.70×10^{-5}, respectively.

(11) The maximum stresses and deformations take place in the area of the triangle. The maximum stresses in TD and LD are 4.65 MPa and 4.82 MPa for PLM and 4.41 MPa and 4.59 MPa for PCM while these stresses for LLM are much less with 1.13 MPa and 0.40 MPa in TD and LD, respectively.

(12) For PLM, the high stresses mainly locate in the middle of photonic crystal structure and do not extend to the remaining laminated layer structures. The minimum stresses are 2.31×10^{-5} MPa and 1.72×10^{-5} MPa in TD and LD, respectively. LLM presents larger stress distribution with the minimum stresses of 1.00×10^{-7} MPa and 1.49×10^{-4} MPa in TD and LD, respectively. In other words, the loads on the first layer influence the whole model. Thus, the photonic crystal structures in the PLM and PCM firstly absorb the energy of the load and reduce the influence of the load on the other layers.

(13) The maximum strains in TD and LD of PLMs are mainly founded in the middle of photonic crystal structure, whereas generally small strains in the other parts. The maximum strains in TD and LD of PLMs are 6.21×10^{-4} and 7.78×10^{-4}, respectively. The maximum strains of PCM are similar to those of PLM. The maximum strains are 1.42×10^{-4} and 7.08×10^{-5} in TD and LD, respectively.

(14) In PLM, the first layer and photonic crystal layer absorb the majority of the energy from the external loads and undergo a large deformation while in the single structural models.

In summary, based on all the compression, tensile and triangular indentation simulation results, it is believed that the mechanical properties of PLM are superior to those of single structural models (PCM and LLM). This is understandable since PLM is most close to the structure of the biological prototype, the elytra of *D. tityus*.

6 Discussions

6.1 Discussions of bio-inspirations from the micro- structure investigations

(1) Bio-inspired materials by mimicking the microstructure of the elytra of *D. tityus* should be anisotropy, as inspired by finding (1) in section **3.1**.

(2) The materials should be a kind of composite and fabricated in layers. Some layer is micro-porous materials for absorbing the energy of the external forces and some layers are not porous materials and the material properties and thicknesses of these layers should be different from each other, as inspired by findings (2) and (3) in section **3.1**.

(3) To enforce the bonding between layers, it is not necessary to use the extra bonding materials between layers. The fibers and fiber bundles can be placed in each layer and cross layers to obtain the bonding force be- tween layers, as inspired by findings (4) and (5) in section **3.1**.

6.2 Discussions of bio-inspirations from the nanoindentation tests

(1) Young's modulus and hardness of the bio-inspired materials should be different between layers, different directions and even at the different locations of each layer. There should be some layers with buffer functions and some layers with high Young's modulus. The changes of Young's modulus and hardness should be continuous between the layers with the same materials, as inspired by findings (1), (2), (4) and (5) in section **3.2.**

(2) The material elasticity of bioinspired composite materials should be distributed in an optimum way, as inspired by finding (3) in section **3.2**.

6.3 Discussions of bio-inspirations from the FEA simulations

(1) If the bio-inspired materials are mainly under the uniform pressure loads in the normal direction to LD, the structural layer design with the uniform layer materials is better than those with different layer materials, as inspired by findings (1) and (3) in section **5.2**.

(2) If the bio-inspired materials are mainly under the dynamic pressure loads, the structural layer design with the different layer materials is better than those with same layer materials. The materials of the top layers should have the capability of absorbing the dynamic external loads, as inspired by finding (4) in section **5.2**.

(3) If the bio-inspired materials are mainly under the axial loads in the direction of LD, the structural layer design with the different layer materials is better than those with the same layer materials if the stress is the main design criteria, as inspired by findings (7) and (8) in section **5.2**. The special attentions have to be paid the bonding between layers, by finding (7) in section **5.2**.

(4) If the bio-inspired materials are mainly under the axial loads in the direction of LD, the structural layer design with the uniform layer materials is better than those with the different layer materials if the strain (de- formation) is the main design criteria, as inspired by finding (9) in section **5.2**.

(5) If the bio-inspired materials are mainly under the complex loads, the structural layer design with the different layer materials is better than those with the same layer materials, as inspired by finding (12) in section **5.2**.

6.4 The limitations

There are some limitations of work presented in this paper, discussed as follows:

(1) For the microstructure investigation work, the friction between fibers and fiber bundles is considered as the main bonding force. In the future, more investigations should be carried out to verify this bonding mechanism and reveal if there are other bonding mechanisms without the requirement of applying adhesives as used in the most existing man-made composites. This is critically important for the design and development of the future bio-inspired composites since the delamination of the composites is still the main problems.

(2) For the indentation tests, the more tests should be carried out to reveal the distributions of both Young's modulus and hardness of the whole body of the elytra of *D. tityus*.

(3) For the three proposed models, the focus is placed only on the different materials, but there is not the consideration of including 'fibers or fiber bundles' in layers and cross layers, which should be considered in the future new models. The factors such as the distributions, fiber sizes and orientations should be included in the new models.

(4) For FEA simulations, the influences of the sizes of mesh elements on the simulation results should be further investigated. The dynamic loads should also be considered.

7 Conclusion

In this paper, *D. tityus* elytra have been selected as the biological prototype for the investigation to obtain the bio-inspirations for the design and development of light and strong materials.

The microstructure investigation and quasi-static nanoindentation tests have been carried out on the ten samples of the selected elytra of *D. tityus* to reveal their mechanical properties and microstructures.

Based on the findings from the microstructure investigation and the nanoindentation tests, three models of bio-inspired materials have been proposed to mimic the seven-layer structure and the different materials in each layer of the elytra of *D. tityus* for further study to gain the deep understanding of the relationships between the special mechanical characteristics and microstructures. A number of FEA simulations have been carried out.

Through comparative analysis of the findings from the microstructure investigation, the nanoindentation tests and the simulations, some meaningful bio- inspirations have been reaped for the future optimization of the design and development of light materials with high ratio of strength to mass.

Acknowledgment

This work was supported by National Natural Science Foundation of China (No. 31672348), National Key R&D Program of China (No. 2016YFE0112100), China-EU H2020 FabSurfWAR project (No. 644971), and by 111 project (No. B16020) of China.

References

[1] Gullan P J, Cranston P S. *The Insects*: *An Outline of Entomology*, 3rd ed, Wiley-Blackwell, New Jersey, USA, 2005.

[2] Vincent J F V, Wegst U G K. Design and mechanical properties of insect cuticle. *Arthropod Structure* & *Development*, 2004, **33**, 87–199.

[3] Vincent J F V. Arthropod cuticle: A natural composite shell system. *Composites Part A*: *Applied Science and Manufacturing*, 2002, **33**, 1311–1315.

[4] Zhang X M, Xie J, Chen J X, Okabe Y, Pan L C, Xu M Y. The beetle elytron plate: A lightweight, high-strength and buffering functional-structural bionic material. *Scientific Reports*, 2017, **7**, 4440.

[5] Zhou Y, Guo C, Zhu C S, Dai Z D. Study on design and mechanics properties of beetle's elytra-inspired lightweight structures with filament winding. *China Mechanical Engineering*, 2011, **22**, 1969–1973.

[6] Zhang F, Gao H, Tong J, Zhou J, Ma Y H. Research on elytron section microstructure of four species beetles and biomimetic models. *Transactions of the Chinese Society of Agricultural Engineering*, 2011, **27**, 105–109. (in Chinese)

[7] Song W W, Guo C, Man Y, Zhang X Y, Dai Z D. Mechanical properties of beetle's elytra-inspired lightweight structures. *Mechanical Science and Technology for Aerospace Engineering*, 2010, **29**, 1376–1379.

[8] Guo C, Song W W, Dai Z D. Structural design inspired by beetle elytra and its mechanical properties. *Chinese Science Bulletin*, 2012, **57**, 941–947.

[9] Xiang J W, Du J X, Li D C, Scarpa F. Numerical analysis of the impact resistance in aluminum alloy bi-tubular thin-walled structures designs inspired by beetle elytra. *Journal of Materials Science*, 2017, **52**, 13247–13260.

[10] Chen J X, Wu G. Beetle forewings: Epitome of the optimal design for lightweight composite materials. *Carbohydrate Polymers*, 2013, **91**, 659–665.

[11] Sun J Y, Tong J, Chen D H, Lin J B, Liu X P, Wang Y M. Micro-tensile testing of the lightweight laminated structures of beetle elytra cuticle. *Advances in Natural Science*, 2010, **3**, 225–234.

[12] Xiang C T, Fan J H. On the strengthening and toughening mechanism of natural composites and research of biomimetic composites. *Advances in Mechanics*, 1994, **24**, 220–232.

[13] Kaufman J D, Klapperich C M. Nanomechanical testing of hydrated biomaterials: Sample preparation, data validation and analysis. *Materials*

Research Society Symposium Proceedings, 2005, **844**, 287–292.
[14] Cuy J L, Mann A B, Livi K J, Teaford M F, Weihs T P. Nanoindentation mapping of the mechanical properties of human molar tooth enamel. *Archives of Oral Biology*, 2002, **47**, 281–291.
[15] Ebenstein D M, Wahl K J. Anisotropic nanomechanical properties of *Nephila clavipes* dragline silk. *Journal of Materials Research*, 2006, **21**, 2035–2044.
[16] Barbakadze N, Enders S, Gorb S, Arzt E. Local mechanical properties of the head articulation cuticle in the beetle *Pachnoda marginata* (Coleoptera, Scarabaeidae). *Journal of Experimental Biology*, 2006, **209**, 722–730.
[17] Lomakin J, Huber P A, Eichler C, Arakane Y, Kramer K J, Beeman R W, Kanost M R, Gehrke S H. Mechanical properties of the beetle elytron, a biological composite material. *Biomacromolecules*, 2011, **12**, 321–335.
[18] Sun J Y, Tong J. Fracture toughness properties of three different biomaterials measured by nanoindentation. *Journal of Bionic Engineering*, 2007, **4**, 11–17.
[19] Oliver W C, Pharr G M. Measurement of hardness and elastic modulus by instrumented indentation: Advances in understanding and refinements to methodology. *Journal of Materials Research*, 2004, **19**, 3–20.
[20] Zhang Z J, Wu W, Tong J, Sun J Y. Relationship of hydration and nanomechanical characteristics of beetle cuticle. *Bio- inspired*, *Biomimetic and Nanobiomaterials*, 2017, **6**, 161–167
[21] Sun J Y, Wu W, Liu C, Tong J. Investigating the nanomechanical properties and reversible color change properties of the beetle *Dynastestityus*. *Journal of Materials Science*, 2017, **52**, 6150–6160.
[22] Rassart M, Simonis P, Bay A, Deparis O, Vigneron J P. Scale coloration change following water absorption in the beetle *Hoplia coerulea* (Coleoptera). *Physical Review E*, 2009, **80**, 031910.
[23] Vincent J F V. Arthropod cuticle: A natural composite shell system. *Composites Part A*: *Applied Science and Manufacturing*, 2003, **33**, 1311–1315.
[24] Wegst U G K, Ashby M F. The mechanical efficiency of natural materials. *Philosophical Magazine*, 2004, **84**, 2167–2186.
[25] Sun J Y, Wu W, Xue W L, Tong J, Liu X P. Anisotropic nanomechanical properties of bovine horn using modulus mapping. *IET Nanobiotechnology*, 2016, **10**, 334–339.